

Vapor–Liquid Equilibrium for the Carbon Dioxide + Hydrogen + Methanol Ternary System

Keivan Bezanehtak, Fariba Dehghani, and Neil R. Foster*

School of Chemical Engineering and Industrial Chemistry, The University of New South Wales, Sydney, NSW 2052, Australia

Vapor–liquid equilibrium data for the ternary system carbon dioxide (CO₂) + hydrogen (H₂) + methanol (MeOH) were determined at temperatures between 278 K and 298 K and pressures between 20 bar and 200 bar. A dynamic technique with vapor and liquid recirculation and on-line gas chromatography was used in this study.

Introduction

Knowledge of the phase behavior of ternary systems consisting of solvent-dense gas-solute is required to optimize the operating conditions of processes such as catalytic hydrogenation reactions. Combes et al.¹ carried out a catalytic hydrogenation reaction for the synthesis of naproxen in MeOH expanded with CO₂ at various temperatures. The ternary system that consists of solvent-dense gas-solute is useful for designing crystallization and fractionation processes.² The conditions at which the reactants maintain solubility in the expanded solution, and at which product precipitates, may be used for simultaneous in-situ synthesis and purification. The pressure and temperature range for which the solubility of a reactant such as H₂ in an expanded solution increases can be established by phase equilibria. This information can then be used in combination with kinetics to increase the yield of the reaction.

The vapor–liquid equilibrium data for the ternary system CO₂ + H₂ + MeOH at 247 K and 228 K were previously measured by Shenderei et al.³ It was found that the H₂ concentration in the liquid phase increased as the total pressure of the system was raised. At pressures above the critical point of the CO₂ + MeOH binary system (30 and 20 bar for 247 K and 228 K, respectively), the H₂ solubility in the liquid phase was significantly increased as the concentration of CO₂ in MeOH increased. At pressures below the critical point of the CO₂ + MeOH binary system, the solubility of H₂ in the MeOH rich phase decreased slightly as the concentration of CO₂ in the ternary system increased. The results obtained by Shenderei et al.³ demonstrate that the solubility of a gaseous component such as H₂ in a solvent can be significantly improved by the addition of CO₂.

The vapor–liquid equilibria for the CO₂ + H₂ + MeOH ternary system have only been previously measured at temperatures below 247 K.³ In this study the vapor–liquid equilibria were measured for CO₂ + H₂ + MeOH for temperatures in the range 278 K to 298 K and for pressures between 20 and 200 bar.

Experimental Section

Materials. Carbon dioxide (industrial grade, 99.5%), hydrogen (high purity, 99.98%), and argon (high purity,

99.997%) were supplied by BOC Gases Australia Ltd. Methanol (99.8 wt %, HPLC grade) was purchased from Mallinckrodt, Australia Pty Ltd.

Apparatus. The dynamic vapor–liquid recirculation apparatus shown schematically in Figure 1 was used to measure the vapor–liquid equilibrium data for the CO₂ + H₂ + MeOH ternary system. A Jerguson sight gauge (series no. 32) with a total volume of 60 cm³ was used as an equilibrium cell. The high-pressure cell allowed visual observation of both the phase behavior and the meniscus. The temperature of the system was controlled with a Unistat 130 heater (Thermoline, Australia Pty Ltd) or a TIC2-581-T cooler (Thermoline, Australia Pty Ltd). The temperature of the equilibrium cell was monitored with a type T thermocouple (standard tolerance ±1 °C) (Pyrosales, Australia), which was calibrated against a precalibrated mercury thermometer and was connected to a digital temperature indicator (Pyrosales). The pressure of the system was measured with a pressure transducer (Druck Limited, PDCR610, 350 bar, precision ±0.1 bar) which was previously calibrated against a hydraulic dead weight tester (Pressurements Ltd). Recirculation of both liquid and vapor phases provided attainment of rapid equilibrium condition in the system. The equilibrium in the system was achieved by recirculating the liquid phase through the vapor phase using a metering pump (Eldex Laboratories, Inc.). The vapor phase was recirculated using a magnetic pump that was designed and constructed in-house.

Carbon dioxide was transferred to the system with a syringe pump (ISCO model 260D), and H₂ was introduced directly into the system via a regulator (BOC Gases Australia Ltd, HPS4-3000-4F-4F). The sampling section has been described in detail previously.⁴

Procedure. The experiments were carried out according to the following procedure. The equilibrium cell was filled with a known amount of MeOH and was then placed in a constant temperature water bath. The temperature of the water bath was controlled using an immersion heater or cooler, and the equilibrium cell temperature was monitored with a type T thermocouple. Carbon dioxide was then gradually added to the equilibrium cell using a syringe pump until the desired pressure was reached. The system was then isolated and equilibrium between the two phases was achieved by recirculating both liquid and vapor phases

* To whom correspondence should be addressed. Telephone: (61) (2) 9385 4341. Fax: (61) (2) 9385 5966. E-mail: N.Foster@unsw.edu.au.

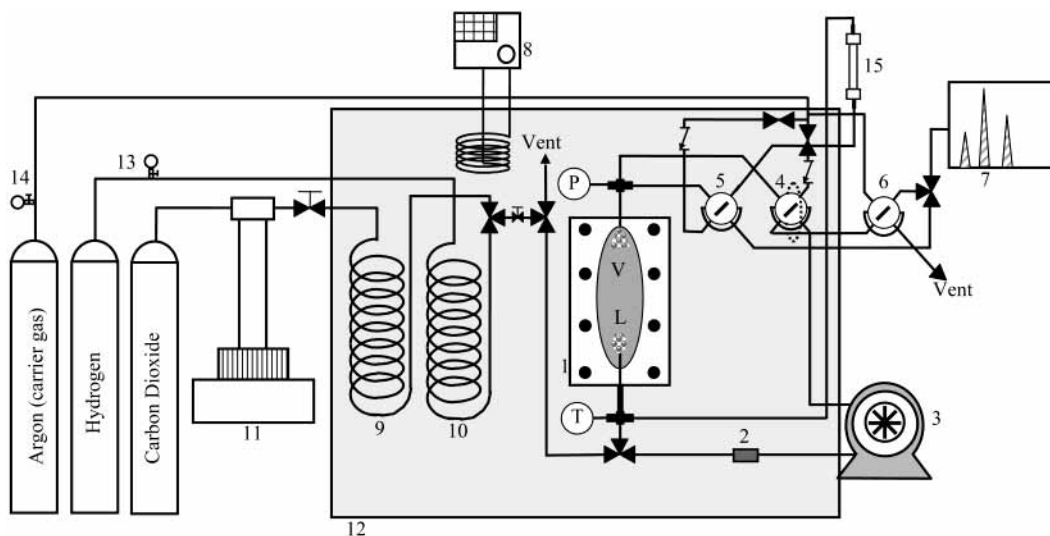


Figure 1. Schematic diagram of the vapor–liquid equilibrium apparatus: 1, equilibrium cell; 2, filter; 3, metering pump; 4, eight-port valve; 5 and 6, six-port valve; 7, gas chromatograph; 8, immersion heater or immersion cooler; 9 and 10, heating coil; 11, syringe pump; 12, water bath; 13 and 14, regulator; 15, magnetic pump.

for at least 4 h using metering and magnetic pumps, respectively.

After equilibrium was established between the two components, the third component (H_2) was introduced into the view cell, via a regulator, until the operating pressure was reached. The system was again isolated and both phases were recirculated until equilibration in the system was attained. Samples from both phases were withdrawn by manipulating the sampling valves and injecting samples into the on-line gas chromatograph. Analyses of the samples from both phases were performed according to the analytical technique described in a previous paper.⁴ A minimum of three samples were withdrawn from both phases for each experimental condition. The relative standard deviation (RSD) of measured compositions was less than 4%.

For each pressure and temperature, tie lines were obtained by utilizing 10 mL of MeOH and varying the relative amounts of CO_2 and H_2 in the equilibrium cell. At high pressure, where the volume expansion of MeOH was dramatic, less MeOH was used to enable visualization of the two phases in the cell.

The reliability of vapor–liquid recirculation system used in this study was confirmed by achieving less than 4.6% absolute average deviation (AAD%) in comparing the data for the binary mixture $\text{CO}_2 + \text{MeOH}$ with the data in the literature.⁴

Results and Discussion

Vapor–liquid equilibrium data for the ternary system $\text{CO}_2 + \text{H}_2 + \text{MeOH}$ were measured at 278 K, 288 K, and 298 K, for various pressures and are presented in Tables 1, 2, and 3, respectively.

At each temperature, vapor–liquid equilibrium data were obtained over three different pressure ranges: below the critical point of the $\text{CO}_2 + \text{MeOH}$ binary mixture, between the critical points of the $\text{CO}_2 + \text{MeOH}$ and $\text{H}_2 + \text{CO}_2$ binary mixtures, and above the critical point of the $\text{H}_2 + \text{CO}_2$ binary mixture.

Range 1: Below the Critical Pressure of the $\text{CO}_2 + \text{MeOH}$ Binary System. The vapor–liquid equilibrium data obtained for the $\text{CO}_2 + \text{H}_2 + \text{MeOH}$ ternary system at 298 K and below 65 bar (the critical point of the $\text{CO}_2 + \text{MeOH}$ binary mixture⁴) are presented in Figure 2a. Each tie line

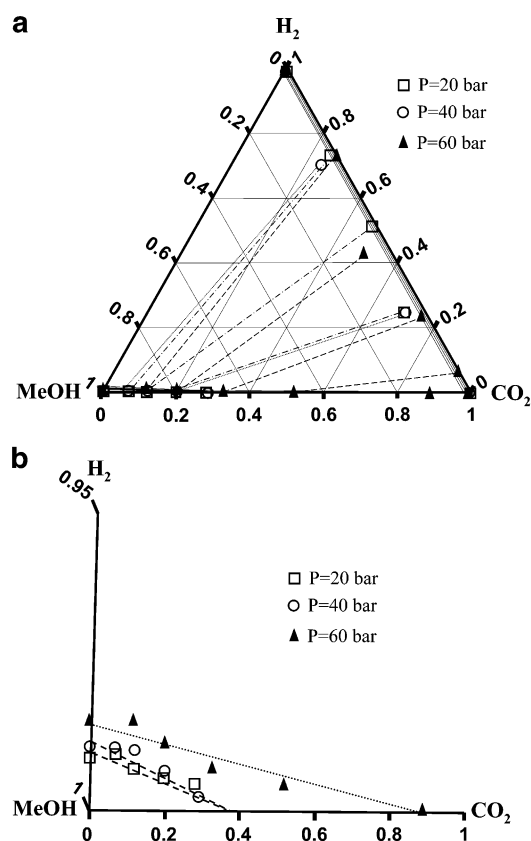


Figure 2. (a) Vapor–liquid equilibrium for $\text{CO}_2 + \text{H}_2 + \text{MeOH}$ (mole fractions) at 298 K and pressures below 65 bar. (b) Enlarged region of the vapor–liquid equilibrium for $\text{CO}_2 + \text{H}_2 + \text{MeOH}$ (mole fractions) at 298 K and pressures below 65 bar (from part a).

in Figure 2a shows the vapor–liquid composition at equilibrium. For each pressure, the liquid solubility line starts from a point on the $\text{H}_2 + \text{MeOH}$ axis in the ternary phase diagram and terminates at a point on the $\text{CO}_2 + \text{MeOH}$ axis. The H_2 solubility in the liquid phase increased as the total pressure of the system was raised due to the high partial pressures of H_2 . As shown in Figure 2b, the liquid miscibility regions were slightly expanded by increasing the total pressure of the system. Hydrogen had negligible

Table 1. Vapor–Liquid Equilibrium Data for the Ternary System CO₂ (1) + H₂ (2) + MeOH (3) at 278 K

x_1	x_2	x_3	y_1	y_2	y_3
$P = 20 \text{ bar; RSD} = 2.3$					
0.0650	0.0033	0.9317	0.2935	0.7065	0.0000
0.1142	0.0028	0.8830	0.4982	0.5018	0.0000
0.1701	0.0012	0.8287	0.7930	0.2070	0.0000
$P = 30 \text{ bar; RSD} = 1.7$					
0.0904	0.0019	0.9077	0.5902	0.4098	0.0000
0.0916	0.0052	0.9032	0.3058	0.6942	0.0000
0.1134	0.0015	0.8851	0.7030	0.2970	0.0000
0.2779	0.0022	0.7199	0.8243	0.1757	0.0000
$P = 39.5 \text{ bar; RSD} = 2.3$					
0.1143	0.0070	0.8787	0.3103	0.6897	0.0000
0.2697	0.0052	0.7251	0.6537	0.346	0.0000
0.4478	0.0031	0.5491	0.8548	0.1452	0.0000
0.4710	0.0020	0.5270	0.9187	0.0813	0.0000
$P = 50 \text{ bar; RSD} = 1.6$					
0.0466	0.0046	0.9488	0.2673	0.7327	0.0000
0.2867	0.0086	0.7047	0.5685	0.4315	0.0000
0.5828	0.0101	0.4071	0.7546	0.2454	0.0000
0.7272	0.0134	0.2594	0.7682	0.2318	0.0000
$P = 70 \text{ bar; RSD} = 0.7$					
0.2549	0.0154	0.7297	0.4052	0.5948	0.0000
0.4191	0.0181	0.5628	0.5526	0.4474	0.0000
0.6053	0.0243	0.3704	0.6100	0.3900	0.0000
0.8196	0.0367	0.1437	0.6335	0.3665	0.0000
$P = 90 \text{ bar; RSD} = 0.8$					
0.2373	0.0153	0.7474	0.4737	0.5263	0.0000
0.2636	0.0222	0.7142	0.3521	0.6479	0.0000
0.3336	0.0202	0.6462	<i>a</i>	<i>a</i>	<i>a</i>
0.4181	0.0252	0.5567	0.5332	0.4668	0.0000
0.5301	0.0336	0.4363	<i>a</i>	<i>a</i>	<i>a</i>
0.7430	0.0494	0.2076	0.5474	0.4526	0.0000
0.8080	0.0542	0.1378	0.5611	0.4389	0.0000
$P = 110 \text{ bar; RSD} = 4.1$					
0.0989	0.0126	0.8885	0.2495	0.7505	0.0000
0.1927	0.0173	0.7900	0.4707	0.5277	0.0016
0.4528	0.0370	0.5102	0.4932	0.5068	0.0000
0.5928	0.0513	0.3559	0.4984	0.5016	0.0000
0.8223	0.0751	0.1026	<i>a</i>	<i>a</i>	<i>a</i>
$P = 130 \text{ bar; RSD} = 0.9$					
0.1549	0.0183	0.8268	0.3141	0.6859	0.0000
0.2724	0.0275	0.7001	0.4094	0.5906	0.0000
0.4760	0.0492	0.4748	0.4568	0.5432	0.0000
0.5912	0.0640	0.3448	0.4628	0.5372	0.0000
0.8404	0.1001	0.0595	0.5214	0.4786	0.0000
$P = 150 \text{ bar; RSD} = 0.5$					
0.2428	0.0293	0.7279	0.3678	0.6322	0.0000
0.2647	0.0316	0.7037	0.3813	0.6187	0.0000
0.5487	0.0639	0.3874	0.4188	0.5812	0.0000
0.6284	0.0823	0.2893	0.4396	0.5604	0.0000
0.7384	0.1007	0.1609	0.4442	0.5558	0.0000
$P = 170 \text{ bar; RSD} = 0.9$					
0.1764	0.0269	0.7967	<i>a</i>	<i>a</i>	<i>a</i>
0.3011	0.0419	0.6570	0.3770	0.6230	0.0000
0.5504	0.0803	0.3693	0.4180	0.5820	0.0000
0.6631	0.1017	0.2352	0.4242	0.5758	0.0000
0.7327	0.1147	0.1526	0.4280	0.5720	0.0000
$P = 200 \text{ bar; RSD} = 1.5$					
0.1640	0.0301	0.8059	0.2637	0.7363	0.0000
0.2523	0.0411	0.7066	0.3373	0.6627	0.0000
0.3788	0.0607	0.5605	0.3826	0.6174	0.0000
0.6662	0.1211	0.2127	0.4074	0.5926	0.0000
0.7298	0.1383	0.1319	0.4135	0.5865	0.0000

^a Vapor-phase mole fraction was not measured under these conditions.

solubility in the liquid phase (<1.5 mol %). The composition of H₂ in the liquid phase then decreased as the CO₂ concentration increased. The decrease of H₂ solubility in the liquid phase was due to the decrease in partial pressure

Table 2. Vapor–Liquid Equilibrium Data for the Ternary System CO₂ (1) + H₂ (2) + MeOH (3) at 288 K

x_1	x_2	x_3	y_1	y_2	y_3
$P = 20 \text{ bar; RSD} = 3.3$					
0.0621	0.0046	0.9333	0.2842	0.7158	0.0000
0.0798	0.0034	0.9168	0.4125	0.5874	0.0001
0.1371	0.0011	0.8618	0.5796	0.3986	0.0218
$P = 40 \text{ bar; RSD} = 1.0$					
0.0795	0.0082	0.9123	0.2466	0.7533	0.0001
0.1550	0.0065	0.8385	0.4777	0.5228	0.0000
0.2618	0.0041	0.7341	0.7457	0.2543	0.0000
$P = 50 \text{ bar; RSD} = 2.0$					
0.0878	0.0104	0.9018	0.2354	0.7231	0.0415
0.1880	0.0105	0.8015	0.4464	0.5139	0.0397
0.2684	0.0069	0.7247	0.6694	0.3293	0.0013
$P = 70 \text{ bar; RSD} = 1.3$					
0.1971	0.0149	0.7880	0.3948	0.6052	0.0000
0.2890	0.0145	0.6965	0.5360	0.4640	0.0000
0.4076	0.0149	0.5775	0.6627	0.3373	0.0000
0.4423	0.0153	0.5424	0.6879	0.3121	0.0000
0.6922	0.0226	0.2852	0.7610	0.2390	0.0000
0.7214	0.0237	0.2549	0.7624	0.2376	0.0000
$P = 90 \text{ bar; RSD} = 1.3$					
0.1601	0.0207	0.8192	0.2772	0.7228	0.0000
0.2938	0.0217	0.6845	0.4626	0.5237	0.0137
0.3314	0.0225	0.6461	0.4991	0.4801	0.0208
0.4347	0.0256	0.5397	0.5857	0.4143	0.0000
0.4687	0.0261	0.5052	0.6107	0.3893	0.0000
0.5990	0.0340	0.3670	0.6512	0.3488	0.0000
0.7419	0.0462	0.2119	0.6666	0.3334	0.0000
$P = 110 \text{ bar; RSD} = 0.8$					
0.1717	0.0258	0.8025	0.3076	0.6924	0.0000
0.2518	0.0272	0.7210	0.3682	0.6318	0.0000
0.3481	0.0303	0.6216	0.4709	0.5291	0.0000
0.5121	0.0394	0.4485	0.5717	0.4282	0.0001
0.6795	0.0575	0.2630	0.6055	0.3944	0.0001
0.8026	0.0758	0.1216	<i>a</i>	<i>a</i>	<i>a</i>
$P = 130 \text{ bar; RSD} = 1.8$					
0.1784	0.0313	0.7903	0.2385	0.7445	0.0170
0.2221	0.0325	0.7454	0.2949	0.6905	0.0146
0.3511	0.0374	0.6115	0.4320	0.5655	0.0025
0.5755	0.0586	0.3659	0.5461	0.4515	0.0024
0.7761	0.0923	0.1316	0.5758	0.4242	0.0000
$P = 150 \text{ bar; RSD} = 1.3$					
0.1557	0.0355	0.8088	0.2530	0.7470	0.0000
0.2133	0.0378	0.7489	0.2626	0.7374	0.0000
0.3561	0.0444	0.5995	0.4116	0.5884	0.0000
0.5745	0.0706	0.3549	0.5175	0.4798	0.0027
0.7544	0.1069	0.1387	<i>a</i>	<i>a</i>	<i>a</i>
$P = 170 \text{ bar; RSD} = 2.1$					
0.1268	0.0346	0.8386	0.1662	0.8338	0.0000
0.1738	0.0406	0.7856	0.2029	0.7971	0.0000
0.2846	0.0462	0.6692	0.3252	0.6748	0.0000
0.4536	0.0615	0.4849	0.4445	0.5555	0.0000
0.5381	0.0742	0.3877	<i>a</i>	<i>a</i>	<i>a</i>
0.5742	0.0816	0.3442	0.5870	0.4130	0.0000
0.7259	0.1208	0.1533	0.5234	0.4733	0.0033
$P = 200 \text{ bar; RSD} = 2.0$					
0.1568	0.0463	0.7969	0.1632	0.8368	0.0000
0.2987	0.0554	0.6459	0.3180	0.6820	0.0000
0.3719	0.0624	0.5657	0.3822	0.6156	0.0022
0.5145	0.0836	0.4019	0.4601	0.5366	0.0033
0.7285	0.1474	0.1241	0.5102	0.4851	0.0047

^a Vapor-phase mole fraction was not measured under these conditions.

of H₂ resulting from increased CO₂ mole fraction. Similar phase behavior was obtained for the CO₂ + H₂ + MeOH ternary system at 278 K and 288 K, as indicated in Tables 1 and 2, respectively.

Table 3. Vapor–Liquid Equilibrium Data for the Ternary System CO₂ (1) + H₂ (2) + MeOH (3) at 298 K

x_1	x_2	x_3	y_1	y_2	y_3
$P = 20$ bar; RSD = 4.0					
0.0391	0.0039	0.9570	0.2469	0.7354	0.0177
0.0687	0.0027	0.9286	0.4696	0.5158	0.0146
0.1109	0.0007	0.8884	0.6566	0.2373	0.1061
$P = 40$ bar; RSD = 1.1					
0.0657	0.0079	0.9264	0.2400	0.7041	0.0560
0.1194	0.0066	0.8740	<i>a</i>	<i>a</i>	<i>a</i>
0.2019	0.0038	0.7943	0.6954	0.2486	0.0560
$P = 60$ bar; RSD = 1.9					
0.1153	0.0152	0.8695	0.2655	0.7345	0.0000
0.2001	0.0104	0.7895	0.4943	0.4323	0.0734
0.3267	0.0077	0.6656	0.7474	0.2389	0.0136
0.5199	0.0044	0.4757	0.9332	0.0688	0.0000
$P = 70$ bar; RSD = 2.4					
0.1093	0.0151	0.8756	0.2600	0.7107	0.0293
0.2262	0.0140	0.7598	0.4996	0.4441	0.0563
0.4131	0.0116	0.5753	0.7616	0.2162	0.0222
0.4974	0.0101	0.4925	0.8465	0.1396	0.0139
0.6881	0.0126	0.2993	0.8918	0.0996	0.0086
0.8254	0.0165	0.1581	0.9006	0.0871	0.0123
$P = 90$ bar; RSD = 1.7					
0.1191	0.0211	0.8598	0.3077	0.6740	0.0183
0.2697	0.0201	0.7102	0.5594	0.4318	0.0088
0.4847	0.0215	0.4938	0.7306	0.2611	0.0083
0.6549	0.0298	0.3153	0.7815	0.2115	0.0070
0.8042	0.0437	0.1521	0.8177	0.1763	0.0060
$P = 110$ bar; RSD = 0.6					
0.1556	0.0260	0.8184	0.2760	0.6299	0.0941
0.2803	0.0275	0.6922	0.4638	0.4999	0.0363
0.4410	0.0307	0.5283	0.6355	0.3460	0.0185
0.6647	0.0509	0.2844	0.7090	0.2748	0.0162
0.8050	0.0743	0.1207	0.7553	0.2367	0.0080
$P = 130$ bar; RSD = 1.1					
0.1897	0.0311	0.7792	0.3043	0.6358	0.0599
0.3914	0.0397	0.5689	0.5397	0.4365	0.0238
0.6389	0.0650	0.2961	0.6613	0.3295	0.0092
0.7987	0.1000	0.1013	0.8408	0.1414	0.0178
$P = 150$ bar; RSD = 2.3					
0.2284	0.0382	0.7334	0.3425	0.6249	0.0326
0.3463	0.0432	0.6105	0.4888	0.4911	0.0201
0.4571	0.0536	0.4893	0.5653	0.4225	0.0122
0.6269	0.0794	0.2937	0.6305	0.3628	0.0067
0.7613	0.1198	0.1189	0.7641	0.2102	0.0257
$P = 170$ bar; RSD = 1.7					
0.2247	0.0431	0.7322	0.3062	0.6493	0.0445
0.3535	0.0515	0.5950	0.4571	0.5174	0.0255
0.5071	0.0702	0.4227	0.5739	0.4134	0.0127
0.5425	0.0756	0.3819	0.5903	0.3995	0.0102
0.6779	0.1102	0.2119	0.6288	0.3624	0.0088
0.7465	0.1428	0.1107	0.6806	0.2820	0.0374
$P = 200$ bar; RSD = 1.2					
0.1984	0.0513	0.7503	0.2515	0.7237	0.0248
0.2428	0.0528	0.7044	0.3099	0.6541	0.0360
0.2833	0.0557	0.6610	0.3576	0.6205	0.0219
0.3290	0.0592	0.6118	0.4097	0.5740	0.0163
0.4449	0.0733	0.4818	0.5152	0.4731	0.0117
0.5534	0.0953	0.3513	0.5814	0.4049	0.0137
0.6608	0.1298	0.2094	0.6178	0.3698	0.0124
0.7037	0.1568	0.1395	0.6297	0.3584	0.0119

^a Vapor-phase mole fraction was not measured under these conditions.

At 298 K and 288 K, the composition of MeOH in the vapor phase was very low and did not exceed 7.3 and 4.2 mol %, respectively. At 278 K, MeOH was almost immiscible in the vapor phase of the CO₂ and H₂ mixture. As shown in Figure 2a, parallel lines to the H₂ + CO₂ binary axis which are sketched through the data points intersect the CO₂ + MeOH and H₂ + MeOH axis where MeOH had

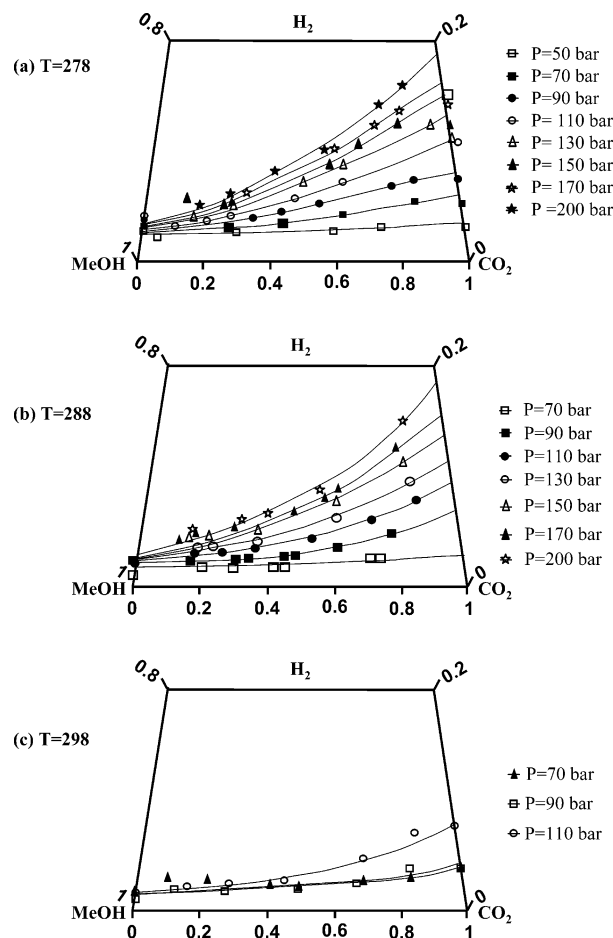


Figure 3. Vapor–liquid equilibrium for CO₂ + H₂ + MeOH (mole fractions) at (a) 278 K, (b) 288 K, and (c) 298 K for pressures above the critical pressure of the CO₂ + MeOH binary system.

very limited solubility in both H₂ and CO₂. Similar behaviors could be obtained for 288 K and 298 K according to the data points listed in Tables 2 and 3, respectively.

Range 2: Between the Critical Pressures of the CO₂ + MeOH and H₂ + CO₂ Systems. Above the critical point of the CO₂ + MeOH binary system, the directions of the liquid lines were different from those of the liquid lines below this pressure, as shown in Figure 3. The liquid-phase lines begin from a point on the H₂ + MeOH axis and extend to the H₂ + CO₂ axis where they intersect at their corresponding binary points. Above the saturated liquid-phase line, a two-phase vapor–liquid equilibrium region exists. The liquid miscibility region expanded as the pressure of the system increased. Hydrogen had very limited solubility in liquid MeOH, and its solubility in the liquid-phase mixture increased with increasing pressure of the system. For example, at 288 K the solubility of H₂ in the liquid phase, at 80 mol % CO₂, was enhanced by 400%, as the pressure of the system increased from 90 to 200 bar.

At each pressure, the H₂ solubility in the liquid phase increased as the concentration of CO₂ in the system increased. The results obtained indicate that the solubility of H₂ was significantly improved in MeOH expanded with CO₂ (252%, 238%, and 160%, respectively) compared with neat MeOH at the same pressure.

The vapor-phase lines at each temperature start from a point on the H₂ + CO₂ axis and intersect the H₂ + MeOH axis at a point corresponding to its binary data point. At low temperatures such as 278 K and 288 K, the vapor-

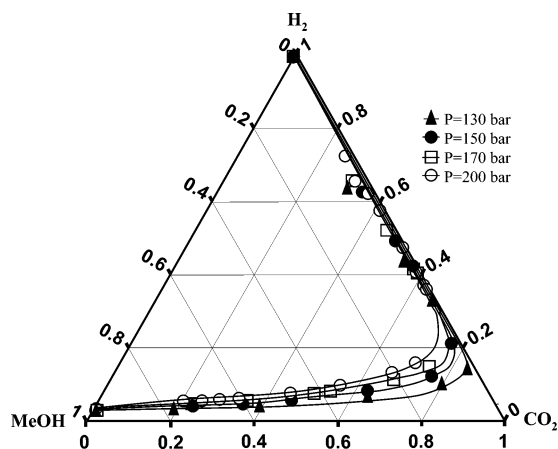


Figure 4. Vapor-liquid equilibrium for $\text{CO}_2 + \text{H}_2 + \text{MeOH}$ (mole fractions) at 298 K and pressures above 120 bar.

phase curves almost superimposed on the $\text{H}_2 + \text{CO}_2$ axis due to the low solubility of MeOH in the vapor phase, as shown in Figure 3a and b. At higher temperatures, 298 K, the MeOH concentration in the vapor phase slightly increased and approached 5.6 mol %, at pressures between 65 and 125 bar (Figure 3c).

Range 3: Above the Critical Pressure of the $\text{H}_2 + \text{CO}_2$ Binary System. In the $\text{CO}_2 + \text{H}_2 + \text{MeOH}$ system, at 298 K, a continuous binodal curve was formed above the critical pressure of the $\text{H}_2 + \text{CO}_2$ binary mixture⁴ (125 bar) for each isobar, as shown in Figure 4. Close to the critical point of the ternary mixture, the concentration of H_2 in the liquid mixture of CO_2 and MeOH increased with increasing pressure. For example, the solubility of H_2 increased from 6.4 mol % to 16.4 mol %, in an expanded MeOH solution containing 70 mol % CO_2 , by raising the pressure of the system from 130 to 200 bar.

Above 125 bar, the concentration of MeOH in the vapor phase was negligible. However, in the vicinity of the critical point of the ternary system, the solubility of MeOH in the vapor phase was slightly higher. It is therefore reasonable to consider the vapor phase as a binary system of $\text{CO}_2 + \text{H}_2$, at pressures below 125 bar, while above 125 bar and in the vicinity of the critical point this assumption is not valid.

Effect of Temperature on the $\text{CO}_2 + \text{H}_2 + \text{MeOH}$ Ternary System. As indicated in Tables 1–3, the solubility of H_2 in the liquid phase increased as the temperature of the system decreased for all pressure regions. For example, the H_2 solubility in expanded MeOH solution (5 mol % CO_2) increased slightly from 0.82 mol % to 0.88 mol % when the temperature decreased from 298 K to 278 K, respectively. The solubility of H_2 in expanded MeOH also increased (at 80 mol % CO_2) by 170% and 436% at 110 bar and 70 bar, respectively, as the temperature of the system was reduced from 298 K to 278 K.

Conclusions

Vapor-liquid equilibrium data for the $\text{CO}_2 + \text{H}_2 + \text{MeOH}$ ternary system were measured at temperatures

between 278 K and 298 K and for pressures up to 200 bar, using a vapor-liquid recirculation apparatus. For all temperatures studied, the solubility of H_2 in the liquid phase increased with increasing pressure. The two-phase region contracted when the pressure of the system was raised. Increasing the temperature reduced the solubility of H_2 in the liquid phase. The liquid-phase region grew larger as the temperature of the system increased.

At all temperatures and pressures below the critical pressure of the $\text{CO}_2 + \text{MeOH}$ binary system, the solubility of H_2 in the liquid phase decreased as the concentration of CO_2 in the system increased. At pressures above the critical pressure of the $\text{CO}_2 + \text{MeOH}$ binary system and below the critical pressure of the $\text{H}_2 + \text{CO}_2$ binary mixture, the solubility of H_2 in the liquid phase was significantly enhanced as the concentration of CO_2 and the total pressure of the system increased.

A distinguishing characteristic of the phase behavior at pressures above 125 bar was the formation of a binodal curve. Close to the critical point of the ternary mixture, the solubility of H_2 in the liquid phase of the $\text{CO}_2 + \text{H}_2 + \text{MeOH}$ ternary mixture was dramatically enhanced as the pressure of the system increased.

At 298 K, the vapor phase consisted mainly of H_2 and CO_2 and the maximum solubility of MeOH in the vapor phase was 4.2 mol %. However, in the vicinity of the critical point of the ternary system of $\text{CO}_2 + \text{H}_2 + \text{MeOH}$ (more than 0.7 mole fraction of CO_2), the solubility of MeOH in the vapor phase was slightly enhanced for all pressures studied. In the vapor phase, the MeOH concentration reached a maximum of 2.1 mol % and 0.2 mol %, at 288 K and 278 K, respectively.

Literature Cited

- (1) Combes, G. B.; Dehghani, F.; Lucien, F. P.; Dillow, A. K.; Foster, N. R. Asymmetric Catalytic Hydrogenation in CO_2 Expanded Methanol – An Application of Gas Anti-solvent Reactions (GASR). *React. Eng. Pollut. Prev.* **2000**, 173–181.
- (2) Warwick, B.; Dehghani, F.; Foster, N. R.; Biffin, J. R.; Regtop, H. C. Synthesis, Purification and Micronisation of Pharmaceuticals Using the Gas Antisolvent Technique. *Ind. Eng. Chem. Res.* **2000**, 39 (12), 4571–4579.
- (3) Shenderei, E. R.; Zelvenskii, Y. D.; Ivanovskii, F. P. Solubility of a Carbon Dioxide-Hydrogen Mixture in Methanol at Low Temperatures Under Pressure. *Khim.-Farm. Promst.* **1961**, 309–312.
- (4) Bezahtak, K.; Combes, G. B.; Dehghani, F.; Foster, N. R.; Tomasko, D. L. Vapor-Liquid Equilibrium For Binary Systems of Carbon Dioxide + Methanol, Hydrogen + Methanol, and Hydrogen + Carbon Dioxide at High Pressures. *J. Chem. Eng. Data* **2002**, 47 (2), 161–168.

Received for review March 20, 2003. Accepted January 2, 2004. The authors wish to thank the Australian Government for financial support through the auspices of the Australian Research Council SPIRT scheme (Biochemical Veterinary Research P/L) (Grant No. C89917624). K.B. wishes to acknowledge the financial support of the Australian Government through the Australian Postgraduate Research Award (Industry) and the Faculty of Engineering, UNSW, for provision of additional financial support.

JE0301491